Measurements and simulations of secondaries with a detector station(s) using CAMAC data acquisition

A Synopsis of the proposed work to be carried out in pursuance of the requirement for the award of the degree

Doctor of Philosophy

In

Physics

Submitted by:

Kajal Garg

Dr. Sonali Bhatnagar
(Supervisor)
Department of Physics & Computer Science

Prof. G.S. Tyagi
Head, Department of Physics & Computer Science

Prof. Ravindra Kumar
Dean, Faculty of Science

Department of Physics and Computer Science
Faculty of Science
Dayalbagh Educational Institute,
Dayalbagh Agra
(Deemed University)
March 2015

1. INTRODUCTION:

Charged particles from the cosmos are continuously coming on the earth; those charged particles are known as cosmic rays. These charged particles have energy from < 1 GeV up to 10^{20} eV, which has been observed till now. Researchers are trying to understand the source of these cosmic rays and their propagation which is a challenge in Astroparticle physics.

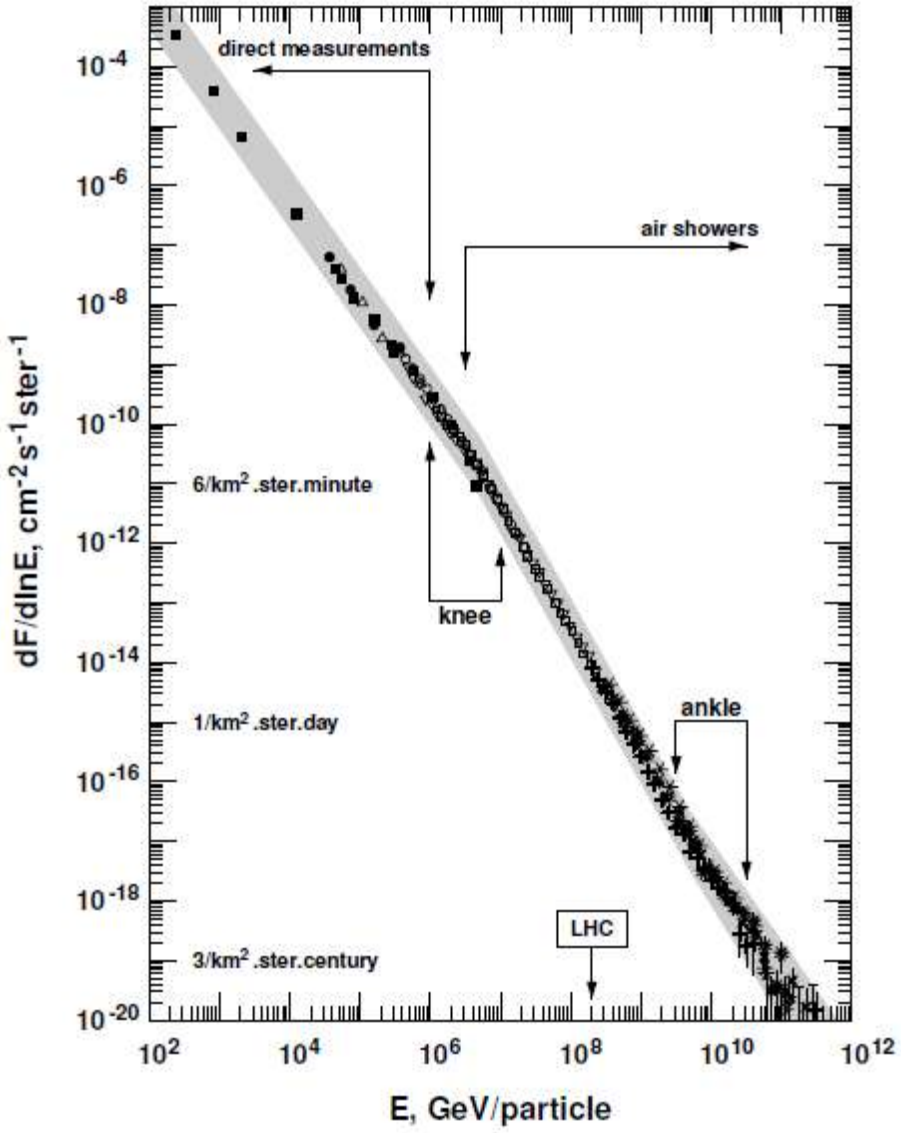

Figure 1: Cosmic ray energy spectrum.

Figure 1 shows the energy spectrum of the cosmic rays. It is a smooth power law spectrum $F(E) = const \times E^{-\alpha}$ with only two identifiable features. The first one is the cosmic ray knee at about 3×10^6 GeV where the spectrum steepens from α = 2.7 to 3.1

and the other one is the ankle, at about 3×10^9 GeV, where the spectrum becomes flat again. The common wisdom is that cosmic rays below the knee are accelerated at galactic supernova remnants. Gamma-rays of energy up to 10 TeV have been observed from sources in the vicinity of well-known supernova remnants which are indication of indeed sources of cosmic ray acceleration. At energy GeV the flux is 1/cm^2/sr/sec/GeV (Stanev1, 2011). Such flux is high enough for direct measurement by using balloon and satellite. At energies above the knee we have no idea about the cosmic ray source, except that the highest energy particles are certainly of extragalactic origin. The acceleration spectra of cosmic rays are considerably flatter (with smallerα) than those of the cosmic rays at Earth. This is believed to be a propagation effect in the Galaxy, where the lower energy cosmic rays are contained for longer time. The first data from the LHC strongly supports the hypothesis that the knee in the cosmic ray spectrum is not caused by the opening of new production channels of unobserved particles or by similar exotic particle physics scenarios. These collider measurements are consistent with the idea that the mixed composition of cosmic rays changes to a heavier composition through the knee-energy range: 10^{15}–10^{16} eV (Ralph Engel, 2011).

1.1.Cosmic ray propagation:

Everything that we know about the propagation of cosmic ray is from the secondaries particles of cosmic rays, gamma rays and synchrotron radiation. Secondary particles are good for observing the cosmic ray propagation because measuring the secondary particles means that secondaries production function can be calculated from cross-sections, primary spectra and interstellar gas densities and then it can be compared with the propagation. Generally the composition is based on primordial solar but for later comparison with solar, it can be defined iteratively from the cosmic rays data themselves (Andrew W. Strong1, 2007).

For a particular particle the cosmic ray propagation equation can be written as

$$\frac{\partial\psi(\vec{r},p,t)}{\partial t} = q(\vec{r},p,t) + \vec{\nabla}.\left(D_{xx}\vec{\nabla}\psi - \vec{V}\psi\right) + \frac{\partial}{\partial p}p^2 D_{pp}\frac{\partial}{\partial p}\frac{1}{p^2}\psi - \frac{\partial}{\partial p}\left[\dot{p}\psi - \frac{p}{3}\left(\vec{\nabla}.\vec{V}\right)\psi\right] - \frac{1}{\tau_f}\psi - \frac{1}{\tau_r}\psi \qquad \ldots\ldots\ldots\ldots\ldots\ldots\ldots\ldots\ldots\ldots\ldots (1)$$

Here $\psi(\vec{r},p,t)$ is cosmic ray density per unit of total particle momentum p at position $\vec{r}$, $\psi(p)dp = 4\pi p^2 f(\vec{p})dp$ in terms of phase-space density $f(\vec{p})$, $q(\vec{r},p)$ is the source term including primary, spallation and decay distribution, D_{xx} is spatial diffusion coefficient (The notion of spatial diffusion covers all processes that contribute to moves, to migration inside geographical space, and to backlash effects generated in this space by those moves), $\vec{V}$ is convection velocity, D_{pp} is diffusion reacceleration which is described as diffusion in momentum space. $\dot{p} = dp/dt$ is momentum gain, τ_f is time scale for loss by fragmentation and τ_r is time scale for radioactive decay.

The spallation part $q(\vec{r},p,t)$ depends on all parent particles and their energy-dependent cross-sections, and the gas density $n(\vec{r})$. In general case it is assumed that the products of such spallation have approximately equal kinetic energy per nucleon as the progenitor. K-electron capture and electron stripping can be included via τ_f and q. D_{xx} is a function of$(\vec{r},\beta,p/Z)$, here $\beta = \frac{v}{c}$ and Z is charge, and p/Z shows the gyroradius in a given magnetic field; D_{xx} may be isotropic or realistically anisotropic and may be influenced by the cosmic rays themselves. D_{pp} and D_{xx} have a relation $D_{pp}.D_{xx} \propto p^2$, the proportionality constant depending on the theory of stochastic reacceleration. The adiabatic momentum gain is represented by the term $\vec{\nabla}.\vec{V}$. τ_f depends on the total spallation cross-section and $n(\vec{r}).n(\vec{r})$ can be based on surveys of atomic and molecular gas. This equation is true only for continuous momentum loss. For catastrophic losses, it included τ_f and q (Andrew W. Strong1, 2007). Progress in cosmic rays research is rapid at the present time with the new generation of detectors for both direct and indirect measurements. But still it is hard to pin-down particular theories and even now the origin of the nucleonic component is not proven, although supernova remants are the leading candidates. The main points we want to make are

• The importance of considering all relevant data, both direct (particles) and indirect (γ-ray, synchrotron) measurements

• Increases in computing power has made many of the old approximations for interpreting cosmic rays data unnecessary

• New high-quality data will require detailed numerical models.

Cosmic ray propagation can be studied in two way either from the *particle* point-of-view, including the spectrum and interactions or treating the cosmic rays as a weightless

collisionless relativistic *gas* with pressure and energy and considering it alongside other components of the interstellar medium. Both ways of looking at the problem are valid up to a point, but for consistency a unified approach would be desirable and to our knowledge has never been attempted. Most papers address exclusively one or the other aspect. The first approach is required for comparison with observations of cosmic rays (direct and indirect) while the second is required for interstellar mass: stability, heating etc. Understanding the composition and spectral features of cosmic rays has always been an astrophysical challenge. On one hand, the observational data have been scarce and suffered from large uncertainties, whereas there are several drawbacks to compare this data with the theoretical predictions.

1.2.Extensive Air Shower:

In the earth's atmosphere when a hadronic high-energy particle interacts with a nucleus from the air (mainly nitrogen, oxygen, and argon) at a typical height of 15 to 35 km, it produces a shower of secondary particles. Neutral pions ($c\tau$ = 25 nm) decay into two photons and charged pions ($c\tau$ = 7.8 m) ($\pi^{\pm} \rightarrow \mu^{\pm} + \upsilon_{\mu}/\overline{\upsilon_{\mu}}$). Charged kaons with a slightly shorter lifetime ($c\tau$ = 3.7 m) decay at higher energies. The secondary particles like baryons, charged pions, and kaons which have long lifetime form the hadronic shower core. π^0 decay into photons which is the dominant source of electromagnetic (EM) shower component. It produces a very small number of hadrons or muons due to photo production. In the hadronic cascade, due to the decay of pions and kaons, 90% muons are produced and propagate through the atmosphere with small energy losses and reach the surface of the Earth almost unattenuated. Muons and electromagnetic components are the only particle which can be detected on the ground, at very large zenith angles ($\theta > 65^{\circ}$). Figure 2 shows the lateral and longitudinal shower profile of different shower components for primary particle (Ralph Engel, 2011). Measuring several observables of air showers allows one to simultaneously probe the overall quality of data description by models. Currently, these estimates are limited mainly to the proton-air cosmic ray cross-section, but they may become much more powerful once independent information about the mass composition of cosmic rays becomes available from magnetic field–deflection patterns or other observations.

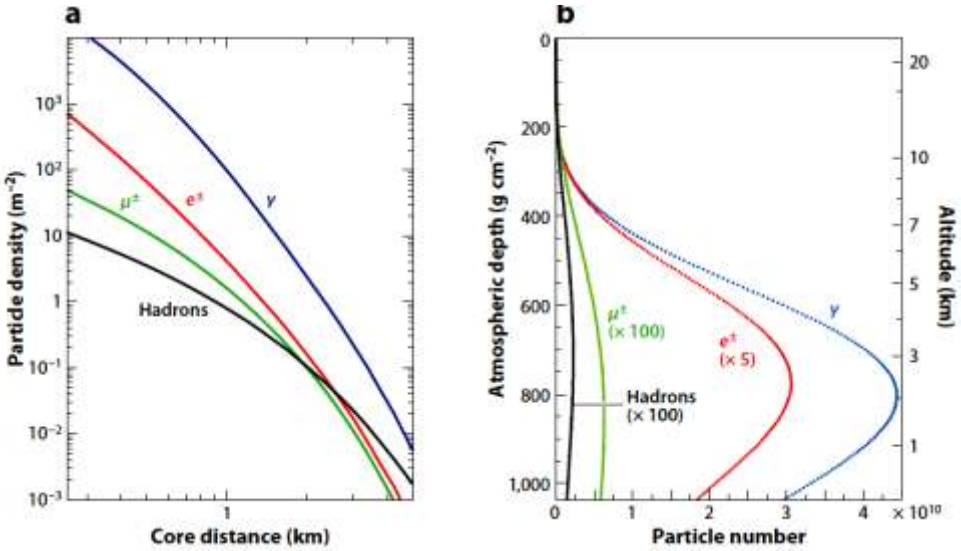

Figure 2:(*a*) lateral and (*b*) longitudinal shower profiles for vertical, proton-induced showers

1.2.1. Electromagnetic Shower:

The basic properties of EM showers follow from the scale invariance of the dominant particle production processes: i.e. pair production, bremsstrahlung and ionization energy. The electron's total energy loss can be given by: $dE/dX = -\alpha\ (E) - E/X_0$, where $\alpha\ (E)$ is ionization energy loss and X_0 is radiation length in air. When the ionization loss is equal to the bremsstrahlung loss, it is considered as the critical energy E_c. Figure 3 shows the EM and hadronic shower.

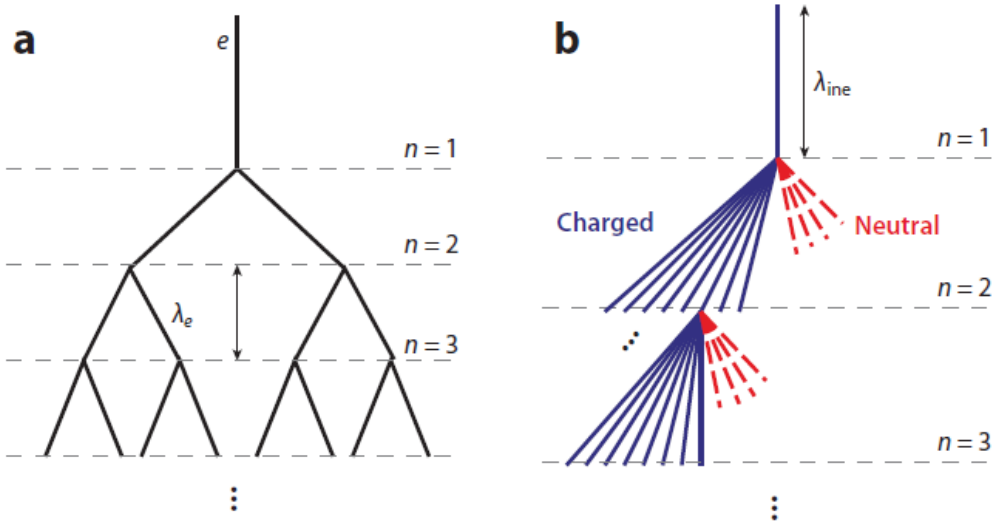

Figure 3: (a) An EM shower, (b) The hadronic Component of a hadron induced shower

The basic features of the longitudinal profile of an EM shower can be understood by the model known as Heitler model. A particle of energy E is considered which produces two new particles having energy $E/2$ for each interaction on traversing a depth λ_e. If n is the number of consecutive interactions, then at a given depth, $X = n \cdot \lambda_e$. Here the number of particles is given by $N(X) = 2^n = 2^{X/\lambda e}$ and the energy of a particle generating n consecutive is given by $E(X) = E_0/2^{X/\lambda e}$, where E_0 is the energy of the primary particle. The particle-multiplication process continues until ionization-energy losses become greater than the radiative losses. The number of particles in the shower reaches the maximum at $E = E_c$, which leads to the following relation:

$$N_{max} = \frac{E_0}{E_c} \; and \; X_{max}^{(EM)}(E_0) \sim \lambda_e \ln\left(\frac{E_0}{E_c}\right) \qquad \ldots\ldots(2)$$

The number of particles at the shower maximum is proportional to *e*nergy of primary particle and the depth of the shower maximum depends logarithmically on the E_0. For example, for photon-induced showers, one obtains

$$\langle X_{max}^{(EM)} \rangle \approx X_0 \ln\left(\frac{E_0}{E_c}\right) + \frac{1}{2} \qquad \ldots\ldots\ldots(3)$$

Multiple Coulomb scattering of electrons leads to the lateral spread of the shower particles. The length scale of the lateral distribution of low-energy particles in a shower is characterized by the Moliere unit $r_1 = \left(\frac{21MeV}{E_c}\right) X_0 \approx 9.3 g cm^{-2}$. Its corresponding

distance in air ais approximately 80 m at sea level, and in cosmic rays extensive air showers with altitude (Ralph Engel, 2011).

1.2.2. Hadronic shower:

For hadron-induced showers also, it is possible to write cascade equations. The difficulty in production of hadronic multiparticle and the need to treat particle decays do not allow for the derivation of analytic expressions for hadronic showers. With the increase in computing power, it has become common to calculate hadronic showers numerically and to parameterize the results. However, some insight into the features of hadronic showers can be gained by generalizing the Heitler model. A hadron of energy E produces n_{tot} total particle during interaction which have energy E/n_{tot}. Among these 2/3 particles are charged pions and 1/3 particles are neutral pion (as shown in **Figure 3b**) which further decay into EM particles ($\pi_0 \rightarrow 2\gamma$). After travelling a distance corresponding to the mean interaction length λ_{ine}, charged particles interact again with air nuclei if their energy is greater than some typical decay energy E_{dec}. Once the energy of the charged hadrons falls below E_{dec}, they produce a muon per hadron. In 'n' time, the energy of hadronic component and EM components can be given as

$$E_{had} = \left(\frac{2}{3}\right)^n E_0 \quad and \quad E_{EM} = \left[1 - \left(\frac{2}{3}\right)^n\right] E_0 \qquad \ldots\ldots\ldots\ldots (4)$$

The depth of the shower maximum of a hadronic shower is determined by the EM particles as shown in **Figure 2*b***. Considering only the EM subshowers produced in the first hadronic interaction, one can write

$$X_{max}^{(had)}(E_0) \approx \lambda_{ine} + X_{max}^{(EM)}\left[\frac{E_0}{2n_{tot}}\right] \sim \lambda_{ine} X_0 \ln\left(\frac{E_0}{2n_{tot} E_c}\right) \qquad \ldots\ldots\ldots\ldots (5)$$

λ_{ine} is hadronic interaction length.

From the charged hadron, number of muons in the Heitler-Matthews is given by

$$E = \frac{E_0}{(n_{tot})^n} = E_{dec} \quad and \quad N_\mu = n_{ch}^n \qquad \ldots\ldots\ldots\ldots (6)$$

If the number of generation (n) is being eliminate than number of muon can be given by

$$N_\mu = \left(\frac{E_0}{(n_{tot})^n}\right)^\alpha \; where\; \alpha = \frac{\ln n_{ch}}{\ln n_{tot}} \approx 0.82 \ldots . 0.94 \qquad \ldots\ldots\ldots (7)$$

The number of muons which will be produced in the air shower it depends upon the primary energy of the shower, the air density, charged and total particle multiplicities of hadronic interactions (Ralph Engel, 2011).

1.2.3. Nuclei and the Superposition Model:

The nucleus mass can be considered because the binding energy of ∼5 MeV per nucleon is much smaller than the typical interaction energies. In this superposition model, a nucleus with mass A and energy E_0 is considered as independent nucleons A with energy $E_h = E_0/A$. This leads to the predictions

$$N_{EM,max}^{(A)}(E_0) = A.N_{EM,max}^{(p)}(E_h) \approx N_{EM,max}^{(p)}(E_0) \quad \dots\dots\dots\dots\dots\dots\dots (8)$$

$$X_{EM,max}^{(A)}(E_0) = N_{max}^{(p)}\left(\frac{E_0}{A}\right), \quad \dots\dots\dots\dots\dots\dots\dots (9)$$

$$N_{\mu}^{(A)} = A.\left(\frac{E_0/A}{E_{dec}}\right) = A^{1-\alpha}.N_{\mu}^{(p)}(E_0) \quad \dots\dots\dots\dots\dots\dots\dots (10)$$

Here (p) and (A) shows the number of particles and shower maximum depth of protons and nucleus induced shower. If the transfer of energy to the EM shower component does not depend upon the energy then there will not be any mass dependence of the number of charges particle at shower maximum. Iron showers contain approximately 40% more muons than proton showers of the same energy, and they reach their maximum 80–100 g cm^{-2} higher in the atmosphere. An important point of this model is that the average of many showers, distribution of nucleon interaction points in the atmosphere coincides with that of more realistic calculations that account for nucleus interactions and for breakup into remnant nuclei.

The cosmic rays quickly interact with the atmospheric molecules, producing an extensive air shower (EAS) that can be considered the superposition of many pion-induced hadronic cascades and electromagnetic showers. Direct methods avoid the secondary particles by flying above the height at which the cosmic rays interact hadronically, while indirect methods measure the secondary particles and radiation produced in the air showers. Satellites and balloons can measure the energy and trajectory of incoming cosmic rays directly, because they lie above the Earth's atmosphere. These techniques boost impressive charge resolution, being able, in some cases, to determine the isotopic abundance, but are limited by the collecting area available (< 5 m^2 sr). Ground-

based telescopes sample the particles or radiation generated in the air showers from primary cosmic rays interacting with the atmosphere. In this way, they can reach a higher energy regime by expanding the collecting area, but are dependent on the hadronic interaction models and have poor charge resolution.

2. LITERATURE REVIEW:

High quality data on the antiproton component could give important clues about the nature of the astronomical dark matter. A very good understanding of the different aspects of cosmic ray propagation is therefore necessary. Propagation is studied with semi–analytical solutions of a diffusion model. It has been recognized for a long time that the relevant physical propagation model to be used are the diffusion model and leaky box model (Maurin, 2011).

(HECK, 2001) Simulated the extensive air shower in CORSIKA (Cosmic Ray Simulations for KAscade) and observed the number of electrons at sea level. 14 % (proton) and 3 % (Fe) at 10^{15} eV become even smaller at lower energies. The differences have shrunk by more than a factor of 3 with respect to a 1997 comparison of the older models. They found out that by the re-evaluation of inelastic proton-air cross sections, a considerable agreement is achieved up to the 10^{7} GeV range. A clear trend of convergence between different hadronic interaction models is obvious for primary energies up to the 10^{6} GeV range. Despite its age, presently QGSJET (Quark Gluon String Model with Joint Engine Technology) still shows the best, though not in all respects satisfying agreement with a variety of experimental results. The new SIBYLL version and the more modern ideas realized in NEXUS (Nuclear Forces Communication Satellite) should enable a more consistent and reliable extrapolation especially to the highest energies.

(A detailed study on nuclear composition of primary cosmic rays around the knee with GRAPES3, 2005), The energy spectra of various nuclei (H, He, N, Al and Fe) and their mean mass have been obtained through a combination of observations on electrons and muons. The mean mass number gradually increases through the *knee* region. These results show dependence on the hadronic interaction models of EAS Monte Carlo. Two models, QGSJET and SIBYLL, were investigated and their results were compared with those from direct measurements. Predictions of SIBYLL agree

with JACEE (Japanese American Collaborative Emulsion Experiment) results, but some discrepancy is seen between QGSJET and JACEE.

There are a large number of mini arrays which are in running stage. Their specification has been given in table1

Table 1: Different mini array/detector station and their specification

Station/Array	**Detector in one station**	**Area of each detector**	**Study**
ALTA (Alberta Large area Time coincidence Array) (Karel Smolek, 2009)	3 (Bicron BC-408 scintillation	0.36 m^2	Search for non-random components of extensive air shower phenomena as evidence by very large area time coincidences
CHICOS (California High School Cosmic Ray Observatory) (R. D. McKeown, 2003)	2 (polystyrene scintillator)	1 m^2	Provide data related to the flux of distribution of arrival direction for Ultra High Energy cosmic rays.
SEASA (Stockholm Educational Air Shower array) (Khaplanov, 2005)	4 (Bicron BC-408 scintillation detector)	0.26 m^2	Variation in count rate related to temperature, pressure, time and angle.
SCROD (*S*chool *C*osmic *R*ay *O*utr each *D*etector) (L.A. Anchordoqui, 2001)	4 (Bicron BCF-91 scintillation detector)	0.9 m^2	Search for long range correlation among air shower occurring at very large separation
HiSPARC (High School Project on Astrophysical Research with Cosmic) (C.Timmermans, 2005)	2 (polystyrene Plastic scintillator)	0.5 m^2	Finding particle density distribution and estimating the energy of events that triggered at least 3 detector stations.
LAAS (Large Area	5 (Bicron BCF-	0.25 m^2	finding the intensity co-relations of Ultra

Air Shower) (Performance of GPS-synchronized EAS arrays in LAAS experiments., 2005)	91 scintillation detector)		High Energy Cosmic Rays
Guwahati University (Nayanmoni Saikiaa, 2005)	8 (Bicron BC 416 plastic scintillator)	2 m^2	Observing local particle density effect of extensive air shower

3. OBJECTIVE:

STEP I: STUDY OF EXTENSIVE AIR SHOWER PARAMETERS

a) Study the Cosmic ray interaction and propagation by numerical simulation.

b) Write the algorithm to study the nuclear composition of cosmic rays at longitude ~ 27.18^{o}N, latitude ~ 78.02^{o}E, altitude ~ 171 m of Agra and simulate extensive air shower parameters using Monte Carlo Simulation package CORSIKA at altitude of Agra.

STEP II: DESIGN, FABRICATE AND SIMULATE THE DETECTOR STATION TO STUDY EXTENSIVE AIR SHOWER.

a) Simulate the primary particle energy vs. detector separation study in a detector station using CORSIKA and Geant4 package at altitude of Agra.

b) Design (adding the wavelength shifting fibres to plastic scintillator), fabrication of the plastic scintillation detectors at Cosmic Ray Laboratory, Ooty and setting up the detector station configuration in an appropriate geometry.

STEP III: CONFIGURATION OF DATA ACQUISITION SYSTEM BASED ON ETHERNET CAMAC CONTROLLER C111C.

a) Configuring the trigger electronics for signal measurements of the EXTENSIVE AIR SHOWER and interface it with CAMAC controller.

b) Calibrate Phillips 16 channel TDC 7187 and Phillips 16 channel ADC 7164 modules with Ethernet C111C CAEN Ethernet controller.

4. METHODOLOGY:

Step I:

a. Cosmic rays diffuse through the galaxy and collide with matter. Measurements of the secondary to primary ratios indicate that CRs are confined until they travel through 1 gm/cm^2 of matter. Their motion can be modeled by the transport equation that states the time-derivative of the number of particles is equal to the sum of a diffusion, energy loss, gain (through re-acceleration), convection, source, spallation and a cascade. The model for propagation is Leaky box model that assumes the evenly distributed sources inject high-energy particles into a volume where they are contained for some time,τ_{esc}, before leaking out of the galaxy. The probability of escape is constant and independent of spatial position. Then the cosmic-ray transport equation reduces to a diffusion term (-N/τ_{esc}), a source term, a spallation term and a cascade term (WISSEL, 2010). Diffusion model give the steady state differential density of the nucleus as a function of energy and position. We need to solve a complete triangular–like set of coupled equations since only heaviest nuclei contribute to a given nucleus. So from these models we'll write the algorithm by which we can study their propagation, interaction and nuclear composition of cosmic rays.

b. The extensive air shower will be simulated in CORSIKA and its parameter will be studied.

Step II:

a. Here we will simulate the extensive air shower and detector station. We'll study the energy vs. detector separation in a detector station using CORSIKA and Geant4 package at altitude of Agra. From the simulation the distance between the detectors will be decided for the altitude of Agra. CORSIKA stands for Cosmic Ray SImulation for KAscade. It is a detailed Monte Carlo program to study the evolution of extensive air showers (extensive air shower) in the atmosphere initiated by various cosmic ray particles (HECK, 2001). Also, prediction of particle energy spectra, densities, and arrival times to be observed in extensive air shower experiments, can be made effectively using CORSIKA Simulation. The Earth's magnetic field affecting the movement of charged particles as well as the atmospheric model to be employed in the simulation depends on the geographic location. CORSIKA provides several atmospheric parameters sets covering the complete climatically and seasonal

influence from tropical, subtropical, and mid-latitude regions to the South Pole. Some more important features are given below (Heck D.)

Interaction models: One of the major uncertainties in Monte Carlo simulation of extensive air shower is the dependence upon the hadronic interaction models. Usually these models are tuned to fit collider data, but unfortunately none of the collider experiments register particles emitted into the extreme forward direction, as they disappear in the beam pipe. These particles carry most of the hadronic energy and are of highest importance in the development of extensive air shower, since they transport a high energy fraction deep into the atmosphere. To estimate the systematic errors due to the hadronic interaction model there are five hadronic interaction models for energies > 80 GeV per nucleon in CORSIKA. Besides the models HDPM (Hadron production based on Detail Parameterization Model) and VENUS (Very Energetic Nuclear Scattering), it also has SIBYLL (An efficient event generator), QGSJET (Quark Gluon Strong model with Joint Engine Technology) and DPMJET (Dual Proton Model with Joint Engine Technology). This enables a systematic comparison of all five models within the environment of the CORSIKA program (Marco Alania, 2009). VENUS, QGSJET, and DPMJET model successfully describes elastic scattering and the total hadronic cross-section as a function of energy. SIBYLL is a minijet model. It simulates a hadronic reaction as a combination of an underlying soft collision in which two strings are generated and a number of minijet pairs leading to additional pairs of strings with higher $p_{\perp}$ endpoints. HDPM is a purely phenomenological model which uses detailed parameterizations of $p\bar{p}$ collider data for particle production. The extensions to reactions with nuclei and to energies beyond the collider energy range are somewhat arbitrary. The Gribov-Regge type models simulate nucleus-nucleus collisions in great detail allowing for multiple interactions of nucleons from projectile and target. HDPM and SIBYLL employ the superposition model assuming an independent reaction for each of the projectile nucleon. QGSJET, DPMJET, and SIBYLL account for minijet production, which becomes dominant at higher energies and leads to increasing cross-sections and more high $p_{\perp}$ particles. While in QGSJET and DPMJET minijets contribute partially to the rise of the cosmic cross-section, they are solely responsible for it in SIBYLL. VENUS is the only model taking into account the interactions of intermediate strings and

secondary hadrons with each other, leading to better agreement with final states as measured in collider experiments at the expense of longer computing times.

The CORSIKA program recognizes more than 50 elementary particles. It gives energy, momentum, location, direction and arrival times of all secondary particles that pass a selected observation level. Particle output is a binary file, which is first decoded to produce a file ASCII (Heck. J., 2011).

The spatial structure of the shower which includes the depth of shower maximum, total energy and mass of primary nucleus, particle swarm due to the combined effect of multiple coulomb scattering and transverse momentum in interactions and decays are studied using CORSIKA. To build a realistic air shower model requires a number of ingredients. The *projectile* particles (primary and secondaries) are virtually known particles which are produced in collisions (nuclei,$p, n, e^{\pm}, \gamma, \mu^{\pm}, \pi^{\pm}, \pi^{0}, K^{\pm}, \rho, \Omega, \Delta, \Lambda, \Sigma$ ...). Their interactions (cross section and particle production) with the nuclei in air and their decay properties need to be known (Marco Alania, 2009).

Step III:

a. CAMAC stands for Computer Automated Machine And Control. CAMAC was designed simply as standard system of transmission of digital data. All communication in the crate is overseen by the module called crate controller. The transmission of the digital signals along with the dataway in a CAMAC crate is performed by TTL logic signals. The table 2 below shows the required signals level for the logic family.

Table 2: Data way signal levels

	Logic 0	**Logic 1**
Input must accept	+2.0 to 5.5 V	0 to +8.0V
Output must generate	+3.5 to 5.5 V	0 to +0.5V

The dataway is the nervous system of CAMAC system. It contains a series of parallel wires running along backplane of the crate connecting each of the slots. Communication between modules, crate controller and host computer is made via the dataway. Three types of wiring make up the data way.

- Power lines
- Busses signal lines
- Point to point lines

Table 3 below shows the CAMAC data way description of signals, symbols and their function.

Table 3: CAMAC Data way signals

Signal	Symbol	Function
Common control signals initialize	Z	Sets module to defined, initial state particularly when power is turned on
Inhibit	I	Disable feature for duration of signals
Clear	C	Clears register and reset flip-flops etc
Look-at-me	L	A signal from a module to the crate controller requesting service or attention. This is a dedicated point to point line. The presence of a LAM may be tested by using function F(8)
Response	Q	A one bit reply signal issued by the module in response to certain commands from the crate controller.
Command accepted	X	Indicate that the module is able to perform the action required by the command.
Busy	B	Indicated dataway operation is in progress.
Timing signal strobe 1	S2	Signal used to control first phase of dataway operation.
Strobe 2	S2	Governs phase 2 of the dataway operation.
Data signals Read	R1-R24	Signals for carrying data from a module.
Write	W1-W24	Signals for carrying data to a module.
Address signals station number	N	Select module in crate
Sub address	A1,2,4,8	Select a specific section of module.
Command signal function	F1,2,4,8,16	Defines the function to be executed by module.

A typical dataway operation generally involves a transfer of signals between a module on one end and the crate controller on the other. The operations which can be made are of two types: command or unaddressed. The command signal must be sent to a specific module so it should be specific and the unaddressed operation involves the issuance of common control signal like initialize, inhibit or clear. Because in the dataway each operation involves a series of signals so synchronization is very important and correct timing must be rigorously maintained in order to assure correct transfer of information. At time t_0, the beginning of the operation, the NAF and B signals are simultaneously activated along with any R or W signals. Timing margins are allowed because it is difficult to have a perfect synchronization between the signals. By time t_1 the NAF and b signal must have reached to the appropriate voltage level. The time between t_1 and t_2, the address module must react and initiate the Q and X status signals. At time t_3 these signals and R or W signals must be at required voltage levels. Here now we see more clearly the significance of the strobe signals S1 and S2. S1 is initiated at t_3 and must be stable by t_4. At this time all the commands and data signals must be settled on their respective lines. At t_6 the strobe s2 is initiated and data or status signals may be changed. Minimum time for a signal CAMAC data transfer is 1μsec. Execution time by the central processor of the computer may be long and can vary from hundreds of microseconds to milliseconds.

b. For the detector station, the electronics which is needed includes power supplies, discriminator, and a coincidence unit. A standard CAMAC based acquisition set-up will be used, which requires a crate, TDC and ADC modules, the crate controller to connect the crate to a PC running an acquisition program. A trigger unit is essential for the realization of coincidence technique in detector station configuration. Cosmic ray experiments which make use of multiple detectors separated by large distances require event time synchronization for the off-line correlation of measured events. The time information on the arrival of each individual event may be used for the reconstruction of extended air showers in large array of detectors, or even to search for possible correlation with other independent installations over huge distances.

5. BIBLIOGRAPHY

A detailed study on nuclear composition of primary cosmic rays around the knee with GRAPES3. (2005). *International Cosmic Ray Conference.* pune.

Performance of GPS-synchronized EAS arrays in LAAS experiments. (2005). *International Cosmic Ray Conference* . Pune.

Andrew W. Strong1, I. V. (2007). Cosmic-ray propagation and interactions in the galaxy. *Arxiv astrophysics*.

C.Timmermans. (2005). Setup and first results of HiSPARC experiment. *International Cosmic Ray Conference.*

CAEN. (n.d.). Technical Information manual of C111C Ethernet CAMAC controller.

Dorman, L. I. (2006). *Cosmic ray propogation, Interaction and Accelaration in space plasma.* Netherland: Springer.

Fowler P.H., C. W. (1957). *The low energy end of the cosmic ray spectrum of alpha-particles.*

G.L, V. (1979). Observations of the galactic magnetic field. Fundamentals of Cosmic physics.

HECK, D. (2001). extensive air shower simulations with corsika and the influence of high-energy hadronicinteraction models. world scientific.

Heck, D. (n.d.). Recent extensons to the sir shower simulation programm CORSIKA.

Heck, J. K. (n.d.). Extensive Air Shower Simulation with CORSIKA, A user guide.

Karel Smolek, F. B. (2009). ALTA. *ICRC.*

Khaplanov, A. (2005). *Performance of the First Detector Station for SEASA.*

L.A. Anchordoqui, J. C. (2001). School Cosmic Ray Outreach Detector (SCROD). *ICRC.*

Leo, W. R. (n.d.). *Techniques for Nuclear And Particle physics experiments.*

Marco Alania, I. J. (2009). Air Shower Simulations. *Cosmic Rays and Astrophysics.*

Maurin, D. (2011). Cosmic Rays below Z = 30 in a diffusion model: new constraints on propagation parameters. *arXiv astro physics.*

Nayanmoni Saikiaa, J. P. (2005). New Experimental set up for UHE Cosmic Ray Detection.

R. D. McKeown, J. G. (2003). CHICOS: Status and Prospects. Universal Academy Press.

Ralph Engel, D. H. (2011). Extensive Air Showers and Hadronic Interactions at high energy. *Annual review of astro physics*.

WISSEL, S. A. (2010). *observations of direct cerenkov light in ground-based telescopes and the flux of iron nuclei at tev energies.* chicago, illinois.

Z.D□bicki, J. K.. (2007). *The Roland Maze Project – Cosmic Ray Registrations at Schools.*